Conductivity and Permittivity Studies in the Diluted Perovskite System $[(NH_3)(CH_2)_6(NH_3)]Fe_xZn_{1-x}Cl_4$, $x = 1$, 0.8, 0.5, and 0

M. F. Mostafa, M. M. AbdelKader, and S. S. Arafat

Physics Dept. Faculty of Science, University of Cairo, Giza, Egypt

Referent requests to Dr. M. F. Mostafa; e-mail: Mohga40@hotmail.com

Z. Naturforsch. **57a**, 897 – 908 (2002); received May 21, 2001

The dielectric permittivity and AC conductivity of the perovskite-like system $[(NH_3)(CH_2)_6(NH_3)]Fe_xZn_{1-x}Cl_4$ ($HDAF_xZ_{1-x}$), where $x = 1$, 0.8, 0.5 and 0, were measured at different frequencies in the temperature range $100\ K < T < 430\ K$. At temperatures below 273 K, for $x = 1$ the material exhibits a transition at (245 ± 1) K, while for $x = 0$ transitions at (155 ± 5) K, (220 ± 4) K and (255 ± 2) K were found. A rotational-type transition in the range 295 – 305 K was found for the Fe-containing materials. Ferroelectric transitions were observed in the high temperature region for all four concentrations. Differential thermal scanning confirmed the existence of the phase transitions above room temperature. The conductivity decreases with Zn addition, an the conduction mechanism varies with the temperature and concentration. Extrinsic conduction prevails for $T < 150$ K for all concentrations. At intermediate temperatures an Arrhenius relation with frequency dependent activation energy ($\Delta E = 0.46 - 0.06$ eV) is observed for Fe-containing materials. The frequency dependent conductivity for all materials has a linear response following the power law: $\sigma_{ac} = A(T) \cdot \omega^{S(T)}$ with the exponent s varying with temperature and composition. At high temperatures, for Zn-rich materials series type conduction with $s \sim 0.6 \pm 0.1$ is identified, while for Fe-rich materials band type conduction prevails. In the low temperature region ionic hopping prevails.

Key words: AC Conductivity; Permittivity Studies; Structure Transitions in Layered Systems.

PACS No: 76, 77

1. Introduction

The two dimensional perovskite layer family $[(NH_3)-(CH_2)_n-(NH3)]MX_4$, $n = 2$, 3,..., M = Mn, Fe, Cu and Cd, X = Cl/Br, has intensively been investigated because of its reduced dimensionality (2- and 1-D magnets), and also because of the existence of numerous structural phase transitions [1 – 6]. The structure consists of infinite sheets made of corner-sharing octahedral MX_6. The cavities between the octahedra are occupied by the terminal NH_3 ends of the alkyl-chains, $[(NH_3)-(CH_2)_n-NH_3]$. They form $N-H\cdots Cl$ hydrogen bonds with the chloride atoms of the octahedra [3, 4].

The sequence and nature of the structural phase transitions are functions of n, M and X. For short chains ($n < 5$, order – disorder transitions of the alkylenedimmonium chains are responsible for the phase transitions. In long chain materials, conformational transitions as well as order-disorder phenomena of the chains exist.

The compounds with M = Zn are some what different when compared to the other members of the series in that [6]:

1. There are no two dimensional macroanions formed by the MCl_4 octahedra; instead one has unassociated $ZnCl_4$ tetrahedra.
2. the chains are intercalated. These differences were also noted in the $[N(CH_3)_4]_2ZnCl_4$, which is also known to have numerous structural phase transitions, some of which exhibit ferroelectricity [8, 9]. A list of the transition temperatures for some members of the $[NH_3-(CH_2)_n-NH_3]MX_4$ family and $[N(CH_3)_4]_2ZNCl_4$ are shown in Table 1.

Because of these differences with other members of the family it seems of a great interest to investigate the effect of introducing the Zn ion in place of the Fe ion in $[NH_3-(CH_2)_6-NH_3]MX_4$ and to study its effect on the layer formation and hence on the phase transitions. This investigation was performed through

0932-0784 / 02 / 1100–0897 $ 6.00

Table 1. List of the transition temperatures T_{tr} (K) for selected materials.

Compounds formula	T_{tr} (K)	Ref.
$(CH_2)_3(NH_3)_2FeCl_4$	230	[2]
$(CH_2)_5(NH_3)_2MnCl_4$	382	[3]
$(CH_2)_5(NH_3)_2PbCl_4$	323	[4]
$(CH_2)_3(NH_3)_2CdCl_4$	373	[3, 5]
$(CH_2)_4(NH_3)_2CdCl_4$	335, 358, 362, 366	
$(CH_2)_5(NH_3)_2CdCl_4$	331, 412	
$(C_5H_{11}NH_3)_2ZnCl_4$	256, 303, 347, 436	[6]
$(CH_2)_6(NH_3)_2FeCl_4$	242	[2]
$[N(CH_3)_4]_2ZnCl_4$	155, 168, 275, 280, 296	[7]
$[N(C_2H_5)_4]_2ZnCl_4$	227	[8]

measurements of the electric properties as a functions of temperature and frequency, and supported by differential thermal analysis. Thus we report the preparation of the $n=6$ system, namely $[NH_3–(CH_2)_n–NH_3]Fe_xZn_{1-x}Cl_4$, $x=1$, 0.8, 0.5 and 0, where both rotational and conformational transitions are likely to take place.

AC dielectric and conductivity measurements as functions of temperature (100 – 430 K) and frequency (20 Hz – 20 kHz), and differential thermal scanning (DSC) as confirmation of the electric results, will be presented.

2. Experimental

2.1. Sample Preparation

The material was prepared by mixing molar ratios of hexanediammonium chloride and the corresponding metal chloride in acidified alcoholic solution. The mixture was heated to 90 °C for one hour in a stream of dry nitrogen atmosphere, then cooled gradually to room temperature while still under nitrogen. Greenish yellow powder precipitated. The material was recrystallized from a mixture of alcohol and ether, then dried under vacuum. The chemical analysis was carried out at the microanalysis unit at the University of Cairo. It showed that the compound has the correct chemical formula.

2.2. Differential Scanning (DSC) Measurements

DSC between room temperature and 200 °C was performed on a Shimadzu (50) differential scanning analyzer with a scanning speed of 5 °C/min. The results could be obtained at temperatures above room temperature only. The data were calibrated with the melting transition of Indium at 157 °C.

2.3. Electric Measurements

The samples were measured in the form of pellets pressed under 2 tons/cm^2 each of 8 mm diameter and 1.0 mm thick. The measuring technique is discussed in [10]. The pellets were coated with silver paste to ensure good electrical contact. The permittivity was measured while heating up the sample in the temperature range 100 – 450 K and the frequency range 20 Hz – 20 kHz.

3. Results and Discussion

3.1. Thermal Analysis

Differential thermal scanning thermographs of the four samples with $x=1$, 0.8, 0.5 and 0 are shown in Figs. 1a, 1b, 1c and 1d, respectively. Several sharp endothermic peaks are observed between room temperature and 470 K for every studied concentration. Besides, small anomalies are also observed as indicated by the arrows in Figure 1. Table 2 lists the transition temperatures as obtained from the different thermographs. The table lists the transitions in the temperature range pertinent to the electric measurements only i.e. in the range between room temperature and 375 K.

Table 2. List of transition temperatures as obtained from DSC for $[(NH_3)(CH_2)_6(NH_3)]Fe_xZn_{1-x}Cl4(HDAF_xZ_{1-x})$ where $x=1$, 0.8, 0.5 and 0.

x	T_1 (K)	T_2 (K)	T_3 (K)
1.0	321 ± 3	295 ± 2	
0.8	348 ± 2	330 ± 4	295 ± 3
0.5	332 ± 3	305 ± 3	
0.0	333 ± 2		

Transition temperatures ≥ 375 K are not included in the table, but are shown in Fig. 1.

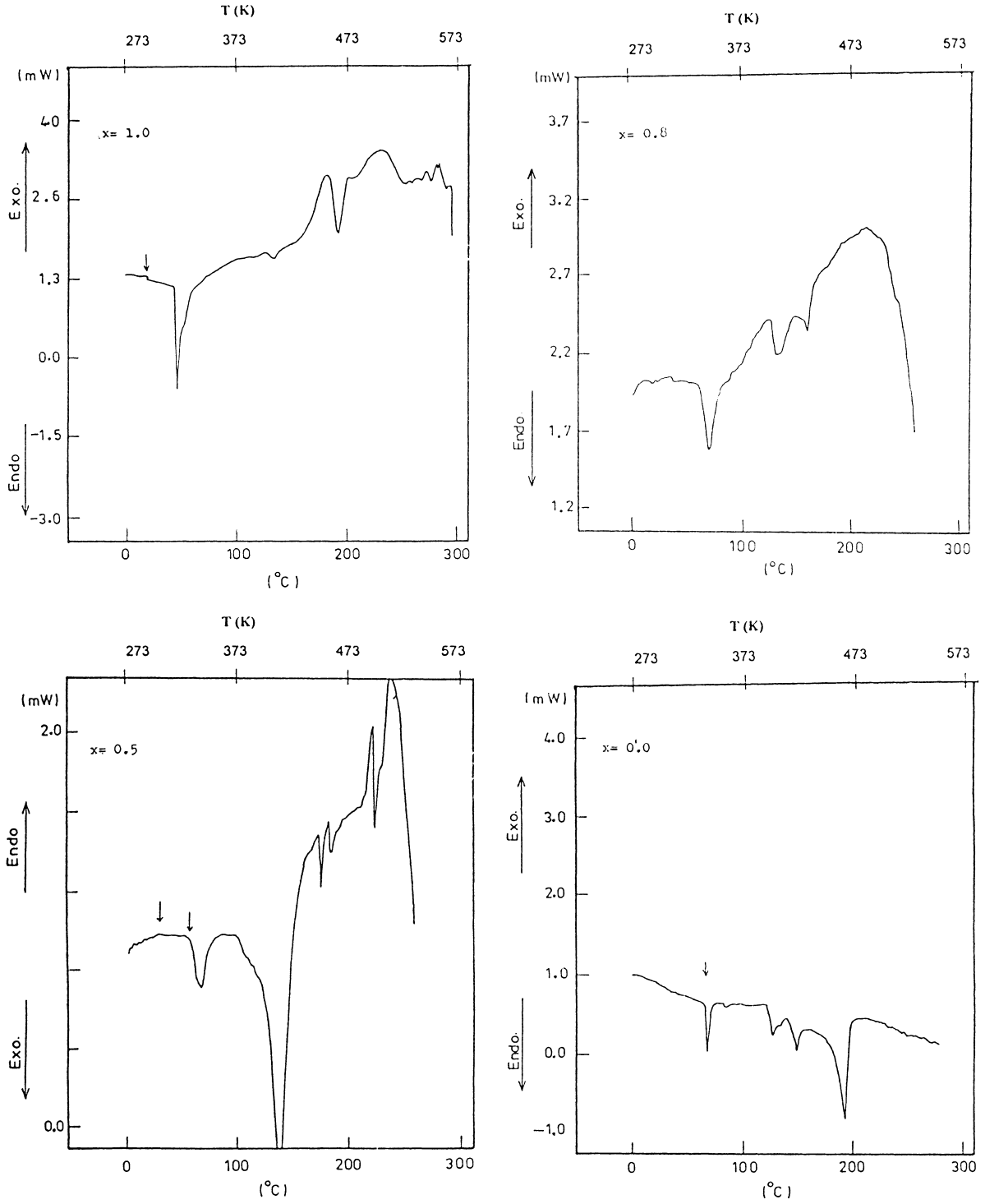

Fig. 1. a) Differential scanning thermograph for $x = 1.0$ (HDAF). b) Differential scanning thermograph for $x = 0.8$ ($HDAF_{0.8}Z_{0.2}$). c) Differential scanning thermograph for $x = 0.5$ ($HDAF_{0.5}Z_{0.5}$). d) Differential scanning thermograph for $x = 0.0$ (HDAZ).

3.2. Dielectric Permittivity

3.2.a) $[NH_3–(CH_2)_6–NH_3]FeCl_4$, $x = 1.0$: (HDAF) results:

Figure 2a shows the variation of the real part of the complex dielectric permittivity presented as ($\ln\varepsilon'$) vs. temperature ($100\ \mathrm{K} < T < 330\ \mathrm{K}$) measured at different frequencies for HDAF. For clarity only six frequencies are depicted. Anomalous variations in permittivity are associated with three transitions at $T_3 = (245 \pm 1)$ K, $T_2 = (295 \pm 3)$ K and $T_1 = (318 \pm 3)$ K, as indicated by the arrows. The large value of ε' and its frequency dependence is likely to be associated with a ferroelectric phase transformation. The anomaly at 295 K is typical for a rotational type transition [11, 12]. The behavior of the temperature dependence of the imaginary part (ε'') is quite similar to that of (ε') except that the order of magnitude of (ε'') is much greater than (ε') at the indicated transitions. The DSC thermograph, Fig. 1a, reveals a small anomaly around 295 K and a sharp endothermic peak at ~ 321 K, which confirms our results. Furthermore, the presence of structural phase transitions at T_3 and T_2 has been confirmed by Mössbauer studies [2, 13].

3.2.b) $[NH_3–(CH_2)_6–NH_3]Fe_{0.8}Zn_{0.2}Cl_4$, $x = 0.8$ ($HDAF_{0.8}Z_{0.2}$) results:

The relation between the real part (ε') of the dielectric constant for this diluted compound, as ($\ln\varepsilon'$) vs. temperature, measured at different frequencies is shown in Fig. 2b. The sharp asymmetric peak found at (348 ± 3) K is associated with shoulders at $\sim(3191 \pm 3)$ K and (295 ± 4) K as well as two frequency dependent peaks at (237 ± 3) K and (154 ± 3) K.

3.2.c) $[NH_3–(CH_2)_6–NH_3]Fe_{0.5}Zn_{0.5}Cl_4$, $x = 0.5$ ($HDAF_{0.5}Z_{0.5}$) results:

The thermal variation of the real part of the dielectric permittivity, as ($\ln\varepsilon'$), obtained at different frequencies is shown in Fig. 2c. The sharp transition at $T_1 = (334 \pm 2)$ K is not symmetric with a change in the slope at $T_2 \approx (303 \pm 2)$ K. The insert depicts a small anomaly in ε' at $T_3 = (160 \pm 5)$ K, characteristic of a rotational type transition. The DSC thermograph reveals good agreement for the high temperature region.

It is to be noted that, for clarity, the inserts of Fig. 2c shows the permittivity ε' rather than $\ln\varepsilon'$.

Table 3. List of transition temperatures as found from the permittivity results for $[(CH_2)_6(NH_3)_2]Fe_xZn_{1-x}Cl4$, $x = 1$, 0.8, 0.5 and 0.

x	T_1 (K)	T_2 (K)	T_3 (K)	T_4 (K)	T_5 (K)
1.0	318 ± 2	295 ± 3	245 ± 1		
0.8	348 ± 1	319 ± 3	295 ± 4	237 ± 4	154 ± 3
0.5	334 ± 2	303 ± 2	160 ± 5		
0.0	337 ± 3	255 ± 2	220 ± 4	155 ± 5	

3.2.d) $[NH_3–(CH_2)_6–NH_3]ZnCl_4$, $x = 0.0$ (HDAZ) results:

The thermal variation of the real part of the dielectric component as ($\ln\varepsilon'$) obtained at different selected frequencies is shown in Fig. 2d. Four anomalies are noted at $T_4 = (155 \pm 5)$ K, where a drop in ε' takes place. At $T_3 = (220 \pm 4)$ K a discontinuity in the rate of increase of ε' is noted, at $T_2 = (255 \pm 2)$ K and $T_1 = (337 \pm 3)$ K relatively sharp peaks were observed. Frequency dependence through out the whole temperature range is observed. The peak's intensities decrease and their positions shift as the frequency increases. It is to be noted that the permittivities are much smaller for HDAZ than for HDAF and/or any of the diluted samples.

The permittivity results for the studied concentrations indicate:

1. Structural phase transitions for the HDAZ at 155 K and 220 K. The latter are associated with rotational type motion.
2. The anomalies found at 160 – 153 K for Zn-containing materials, namely $x = 0.8$, 0.5 and 0, must be related to the presence of Zn ion. Thus it is possible to suggest that these transitions are related to rotational motion of the $ZnCl_4$ tetrahedra. X-ray investigation of the corresponding $[(CH_3)_4N]_2ZnCl_4$, at low temperature showed rotational motion of $ZnCl_4$ to be associated with a phase transition at 155 K [7].
3. Displacive type phase transition occurs at 245 K for HDAF and at 255 K for HDAZ.

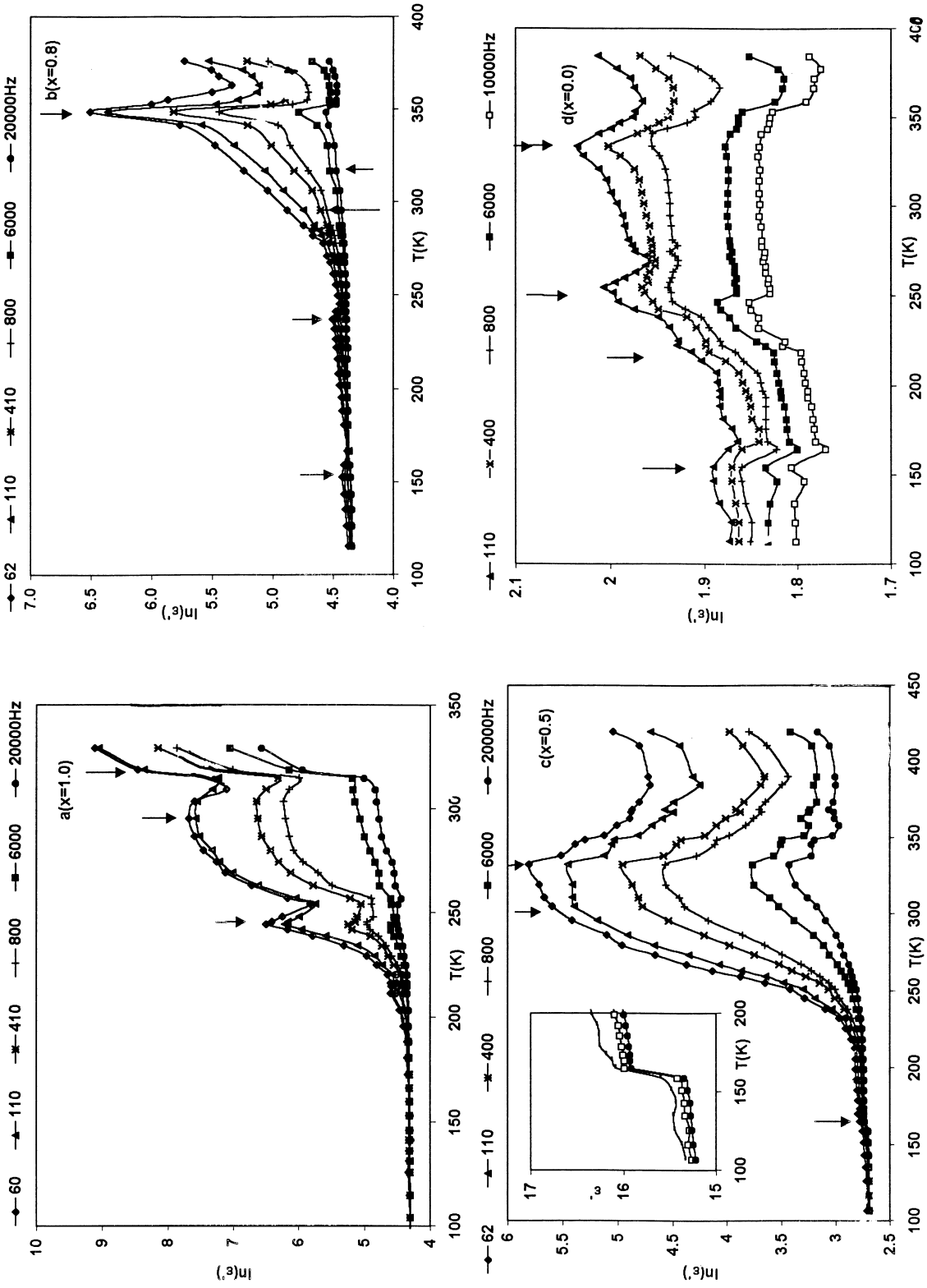

Fig. 2. a) Semilogarithmic representation of the real part of the dielectric permittivity ($\ln\varepsilon'$) vs. temperature for $x = 1.0$ (HDAF) at different frequencies. b) Semilogarithmic representation of the real part of the dielectric permittivity ($\ln\varepsilon'$) vs. temperature for $x = 0.8$ ($HDAF_{0.8}Z_{0.2}$) at different frequencies. c) Semilogarithmic representation of the real part of the dielectric permittivity ($\ln\varepsilon'$) vs. temperature for $x = 0.5$ ($HDAF_{0.5}Z_{0.5}$) at different frequencies. d) Semilogarithmic representation of the real part of the dielectric permittivity ($\ln\varepsilon'$) vs. temperature for $x = 0.0$ (HDAZ) at different frequencies.

4. All Fe-containing samples ($x = 1$, 0.8 and 0.5) show characteristic phase transitions in the range 295 – 303 K. Thus one may relate these phase transitions to the layered structure that is present in the Fe-containing material. This transition is related to a rotational type of motion of the two terminal NH_3-groups: A change in the bonding scheme from "orthorhombic", where hydrogen bonding takes place between two corner sharing equatorial chlorides, and one axial to a "monoclinic" bonding scheme, where two nonbonding axials and one equatorial chloride ions are involved [3].
5. At higher temperatures a characteristic temperature for a phase transition of Zn-rich materials appears at ~ 337 K (at $f = 110$ Hz).

3.3 Dielectric Modulus

The observed frequency dispersion of the permittivity arises from the electrode polarization, which is determined by technical factors, e.g. sample dimension and/or the nature of the electrode surface. Macedo et al. [14] have introduced the electrical modulus $M^* = 1/\varepsilon^*$ to overcome the effect of electrode polarization. $M^* = M' + iM'' = \{1/\varepsilon'(1 + \tan \delta^2)\} + \{i \tan \delta/\varepsilon''(1 + \tan \delta^2\}$. The imaginary part M'' of the complex electric modulus does not include the contribution from the electrode effect.

It is to be noted that both $M^*(f)$ and $\sigma^*(f)$ are derived from the same experimental data (i.e., real and imaginary components of the sample impedance). However, as has been recognized [15], the shape of the modulus is sensitive to $\varepsilon(\infty)$, the high frequency limiting permittivity that results from near instantaneous electronic and atomic polarization, which is not directly related to the hopping motion of the mobile ions. A contribution to $\varepsilon_{\text{total}}$ comes from the Maxwellian dc conductivity ε_c, as well as from relaxation processes ε_r [16]. In order to separate the contributions due to relaxation, one must subtract ε_c. This is done by extrapolating $\ln\sigma$(Gw) to the limit of $\omega = 0$, from which one obtains σ_{dc} values. Substituting into the relation $\varepsilon_c = \sigma_{dc}/\varepsilon_0\omega$, one obtains ε_c. The $\varepsilon_r = \varepsilon_{\text{total}} - \varepsilon_c$ values are used to calculate M' and M''.

The frequency dependence, at different temperatures, of the real M' and imaginary M'' parts of the complex dielectric modulus as functions of the frequency ($\ln\omega$) are shown in Figs. 3a up to 3f for $x = 1$, 0.8, and 0.5, respectively. The plots show features of ionic conductors, namely an S shaped dispersion in M' and a peak in M''. The relaxation peak moves through the temperature "window" or frequency "window" as the temperature and/or frequency changes. It is to be noted that although the peak shifts its position, its amplitude is unaffected by temperature or frequency. The frequencies of the maxima are plotted versus the reciprocal temperature for each of the three materials as seen in Fig. 3g – 3i. Relaxation behavior can be analzyed assuming the simple exponential activation law:

$$f = f_0 \exp(-E_a/kT), \tag{1}$$

which yields the activation energy 0.44 eV, 0.64 eV and 0.63 eV for $x = 1$, 0.8 and 0.5, respectively. This indicates that the addition of Zn ion causes an increase in the activation energy of relaxation.

3.4. AC Conductivity

3.4.1. Temperature Dependence

3.4.1.a) $x = 1$ (HDAF) results:

The AC conductivity plotted as $\ln\sigma$ vs. $1000/T$, measured at different frequencies is shown in Fig. 4a. Several temperature regions may be identified. In region (I)a frequency dependent, temperature independent behavior reflects an extrinsic type conductivity. In region (II), the conductivity is temperature and frequency dependent and increases with increasing frequency and temperature. Regions denoted "T" on all plots refers to a transition region. The number of data points in these regions are limited, hence no meaningful calculations are possible. Region III ($250 \text{ K} < T < 295$ K) is characterized by a thermally activated behavior with both the conductivity (σ) and activation energy (ΔE) being frequency dependent with values of $\Delta E = 0.44 - 0.27$ eV. The values of ΔE are in the range found for protonic hopping [16]. Finally regarding region IV ($T > 300$ K), there are not enough data points to calculate activation energies. However it is likely that the conduction is of Arrhenius type.

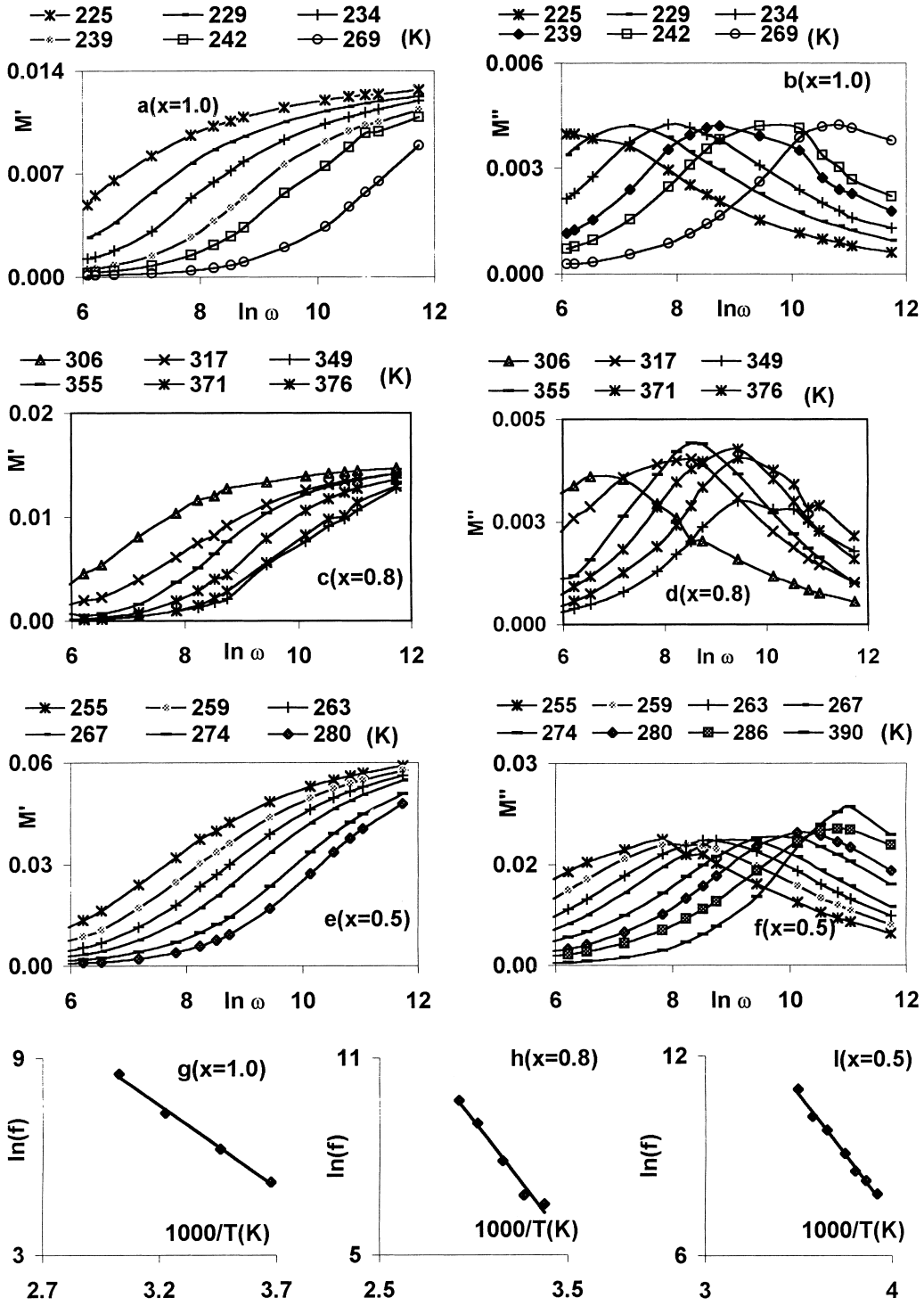

Fig. 3. a, b) Real part (M') and imaginary part (M'') of the dielectric modulus vs. frequency for $x = 1.0$ (HDAF) at different temperatures, lines are guide to the eye, c, d) Real part (M') and imaginary part (M'') of the dielectric modulus vs. frequency for $x = 0.8$ ($HDAF_{0.8}Z_{0.2}$) at different temperatures, lines are guide to the eye, e, f) Real part (M') and imaginary part (M'') of the dielectric modulus vs. frequency for $x = 0.5$ ($HDAF_{0.5}Z_{0.5}$) at different temperatures, lines are guide to the eye, g) ln (frequency) vs. $1000/T$(K) for $x = 1.0$, lines are fit to (1), h) ln (frequency) vs. $1000T$/(K) for $x = 0.8$, lines are fit to (1), i) ln (frequency) vs. $1000/T$(K) for $x = 0.5$, lines are fit to (1).

3.4.1.b) $x = 0.8$ ($HDAF_{0.8}Z_{0.2}$) results:

The conductivity for $x = 0.8$ as function of temperature and frequency is shown in Fig. 4b. Four regions are also identified. In region (I) extrinsic type conduction prevails. Region (II) (237 – 330 K) follows the Arrhenius relation having different slopes at the different frequencies. In this range $\Delta E = 0.46 - 0.30$ eV, which is nearly the same as that obtained for the $x = 1$ sample. Hence protonic conduction prevails in this temperature range, Region (III) and the region denoted "*T*" are associated with the phase transition regimes, and it is not possible to carry out any meaningful calculations due to the limited number of data points.

3.4.1.c) $x = 0.5$ ($HDAF_{0.5}Z_{0.5}$) results:

Figure 4c shows the conductivity as function of the reciprocal temperature for the $x = 0.5$. Four regions are identified. Region (I), (100 – 235 K) extrinsic type conduction with the very low activation energy ~ 0.004 eV prevails. In region (II), (250 – 295 K), a frequency dependent conductivity that follows the Arrhenius relation is obtained with frequency dependent activation energy $\Delta E = 0.24 - 0.06$ eV. This value of ΔE is also in the range of protonic conduction. No calculations were carried out in region (III) due to the limited number of data points.

3.4.1.d) $x = 0$ (HDAZ) results:

Figure 4d shows the conductivity as function of the reciprocal temperature for the $x = 0$. Several regions are identified. As was found for the Fe containing samples, extrinsic type conduction with a small activation energy of 0.01 eV is found in region (I), (100 – 155 K). Region (II) shows frequency dependent conductivity, however, data are scattered in the light of the existence of structural transition, and no calculations were made in this temperature range. A frequency dependent conductivity with activation energy $\Delta E = (0.17 \pm 0.02)$ eV was found. This is the lowest ΔE, for region (III), among the four studied samples. The Arrhenius relation does not apply in region (IV). The number of data points in region (V) is too limited to allow for any meaningful calculations. Table 4 lists values for activation energies for all samples.

Table 4. List of activation energies as obtained from conductivity measurements.

Sample	*x*	Temperature region (K)	ΔE (eV)
HDAF	1.0	II (250 – 390)	0.44 – 0.2
$HDAF_{0.8}Z_{0.2}C$	0.8	II (237 – 333)	0.46 – 0.3
$HDAF_{0.5}Z_{0.5}C$	0.5	III (250 – 295)	0.24 – 0.06
HDAZ	0.0	IV (222 – 255)	0.17 ± 0.02

Comparison of the conductivity results in the high temperature region for the four samples reveals that the conductivity decreases with addition of Zn. One may relate this decrease in conductivity to the difference in the structure between the layered type matrix in Fe-rich materials and the pseudo layered structure of the Zn-rich materials. As mentioned above, the former contains $FeCl_6$ octahedra that share corners, with two axial chlorides that are weakly bonded by H-type bonds. Thus, at high temperatures it is likely that hopping of these axial chlorides can take place, hence causing an increase in the conductivity as compared to the Zn-rich materials where the number of Cl ions available for hopping is smaller in case of $ZnCl_4$ traheda.

As is clear from the Table 4 the activation energy is nearly the same for the Fe-rich samples and decreases as the Zn concentration increases. Since proton hopping is likely to be the conduction mechanism in the low temperature region, this means that the energy needed for protonic hopping is lower for the Zn-rich than the Fe-rich materials. This is not surprising in the light of their structural differences. As Zn replaces Fe, it causes disruption of the 2-D layer, which leads to lowering of the potential barrier for the hopping protons, thus leading to a decrease in the activation energy.

3.4.2. Frequency Dependence

All studied materials showed frequency dependences. Figure 5a – c show the variation of the conductivity with frequency at different temperatures for $x = 1$, 0.8, and 0.5, respectively. Similar behavior was found for $x = 0$. Most previously studied isomorphous perovskite materials in our laboratory [10, 12], as well as elsewhere [17, 18], were found to follow a power law behavior

$$\sigma_{ac} = A(T)\ \omega^{s(T)}, \tag{2}$$

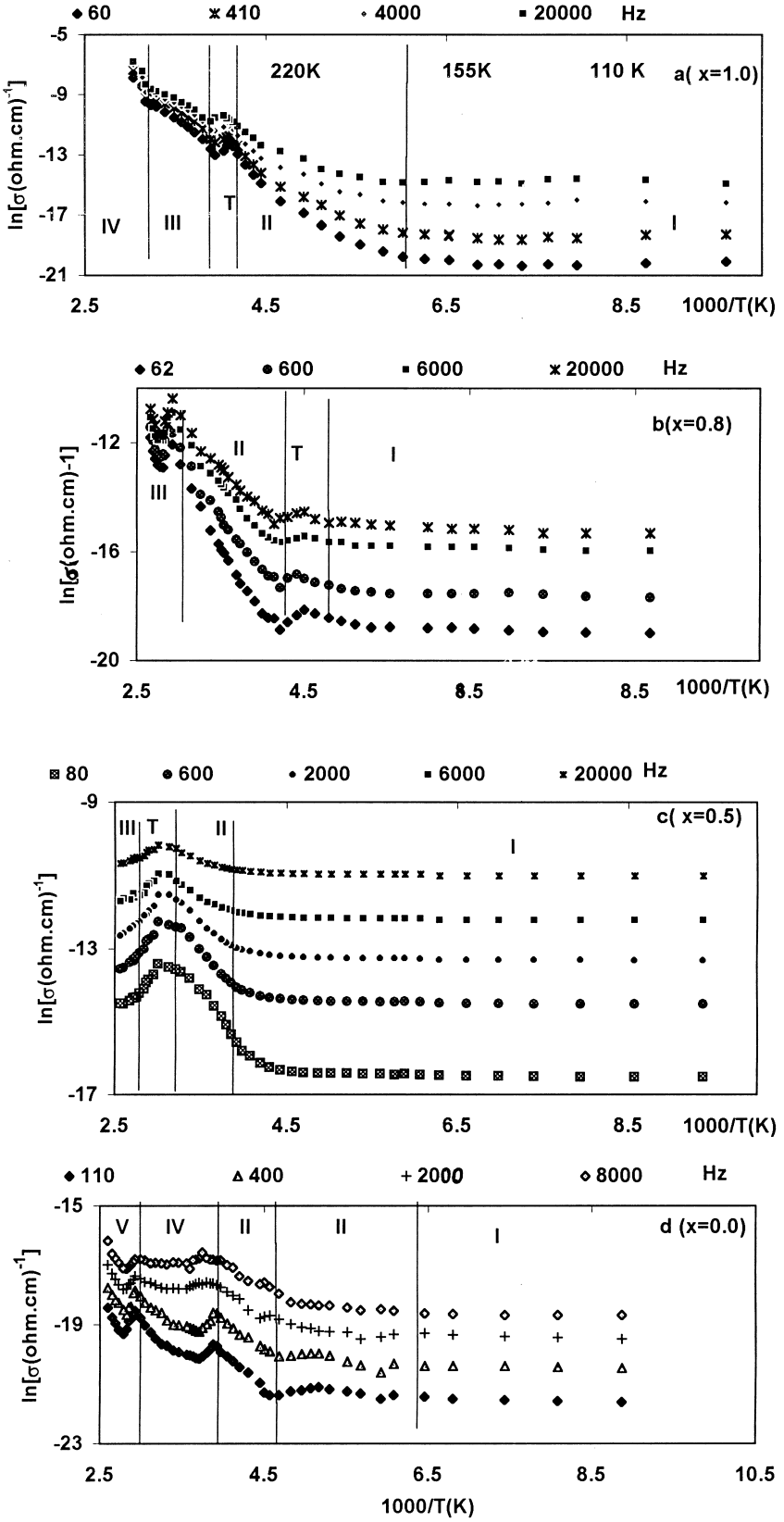

Fig. 4. a) Ac conductivity (σ') vs. reciprocal temperature ($1000/T$(K)) for $x = 1.0$ (HDAF) at different frequencies. b) AC conductivity (σ') vs. reciprocal temperature ($1000/T$(K)) for $x = 0.8$ ($HDAF_{0.8}Z_{0.2}$) at different frequencies. c) AC conductivity (σ') vs. reciprocal temperature ($1000/T$(K)) for $x = 0.5$ ($HDAF_{0.5}Z_{0.5}$) at different frequencies. d) AC conductivity (σ') vs. reciprocal temperature ($1000/T$(K)) for $x = 0.0$ (HDAF) at different frequencies.

where the pre-factor $A(T)$ and the exponent s ($0 < s < 1$) are function of temperature. The relation between σ and ω usually falls on straight lines in the double-logarithmic representation, and the slopes of the lines (the exponent s) are obtained and their variation with temperature is related to the conduction mechanism [17, 19].

To find the type of conduction corresponding to the different temperature regions mentioned above, we have calculated the value of the frequency exponent s by plotting the relation between ln σ and ln (ω) at different temperatures according to the equation $\sigma(\omega) = A\omega^s$, where A is constant. The plots of s vs. T is shown in Fig. 5d – g for $x = 1$, 0.8, 0.5 and 0, respectively. Near 100 K and slightly above it, the exponent s is nearly constant except at the transition temperatures, where anomalies are noted as indicated by arrows. Further increase in temperature is associated with a linear decrease in s. The temperature at which s starts to decrease shifts to higher values increasing Zn content, see Figs. 5d – g. In the high temperature region, for $x = 1$ and 0.8, the obtained values of s show a continuous decrease approaching zero with increasing temperature. On the other hand, for $x = 0.5$ and $x = 0$, s has a constant value of 0.6 ± 0.1. That is, for the Fe-rich to the cryogenic regime s becomes nearly $= 1$. The high temperature region is referred to as the "Jonscher regime", and the $s = 1$ region as the "constant loss regime" [20 – 24], since $\sigma \propto \omega$, $\sigma = \varepsilon_0 \varepsilon'' \omega$ means that ε'' is a constant [25].

There are two basic theories that describe the "Jonscher" type behavior.

i) Independent separate ionic hopping events that have a broad distribution of relaxation times, known as the parallel type conduction mechanism.
ii) Collective effect, where each hopping has strong interactions with surrounding ions (usually Coulombic type), known as the series type conduction mechanism. This mechanism seems to explain better the "Jonscher" behavior.

Therefore we suggest that at high temperatures for the materials with high concentration of Zn ($x = 0.5$ and 0), a series type conduction mechanism prevails, while for high concentration of Fe ($x = 1$ and 0.8) a different type of conduction mechanism prevails. Normal band-type conduction has been found for small values of s, which decreases with increase of temperature [10], thus we suggest that for Fe-rich samples in the high temperature region, band type conduction prevails.

Regarding the constant loss regime, it is usually explained in terms of the pair approximation as introduced by Pollak and Pike [26]. In this model particles or ions occupy one of two positions in an asymmetrical double well in which V is the height of the potential well, Δ is the asymmetry and R is the distance separating the two ions. Several other models based on the pair approximation have been used to account for the conduction mechanism in glass an ionic materials [17, 18]. For example, in the quantum mechanical tunneling (QMT) model the exponent s is given by

$$s = 1 - 4/\ln(1/\omega\tau_0), \tag{3}$$

where τ_0 is the characteristic relaxation time (of the order of the inverse phonon frequency). In this model the ac conductivity is linearly dependent on temperature, and the frequency exponent is temperature independent. For typical values of the parameters, namely $\tau_0 \simeq 10^{-13}$s and $\omega = 10^4 s^{-1}$, a value of $s = 0.81$ is obtained from (3). Although the general trend of s is expected, i.e. temperature independent, yet the values of the calculated τ_0 were found to be $1.33 \cdot 10^{-45}$s, $7.83 \cdot 10^{-10}$s, 1.910^{-178}s and 1.9410^{-9}s for $x =$ 1, 0.8, 0.5 and 0, respectively, thereby conflicting with the prediction of the QMT model. A temperature dependent frequency exponent is obtained for non-overlapping small polarons, however this leads to an increase of s with temperature, which is not the case for these samples. The overlap large polaron tunneling (OLPT) predicts that s should decrease from unity with increasing temperature, reach a minimum then increase in a manner similar to small polarons. We have tried to fit the sample with $x = 0.5$ over the whole temperature range to such a model, however the fit was very poor. Thus it is best to describe the conduction for $x = 1$, 0.8 and 0.5, to be due to hopping. As mentioned above, values of activation energies calculated lie in the range of proton hopping, therefore we suggest that this is the type of mechanism for these three materials. It is not possible to investigate the type of conduction for the HDAZ in the low temperature range due to the consecutive variations in s as a result of the many structural phase transitions observed in this temperature regime.

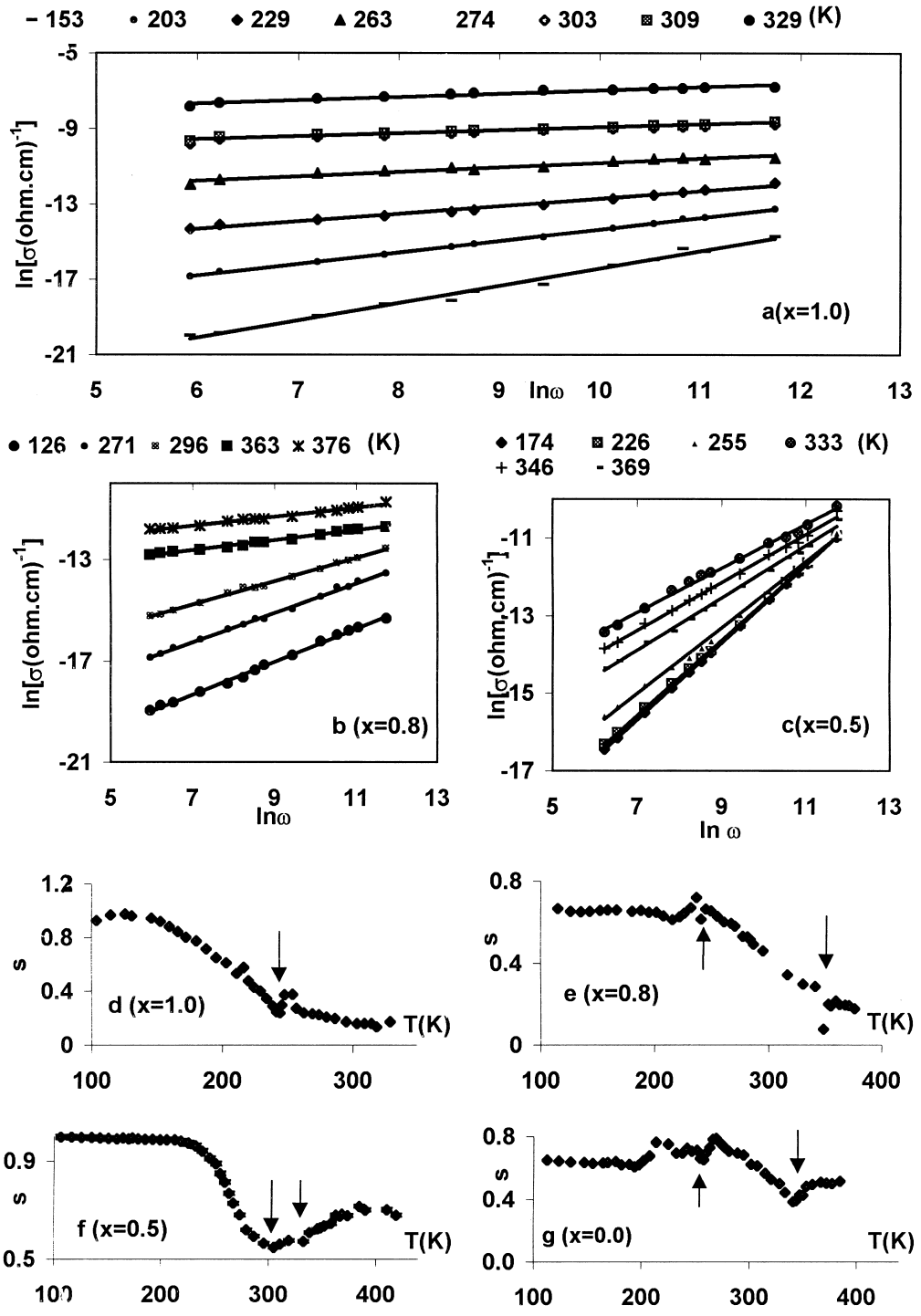

Fig. 5. a) AC conductivity (σ') vs. frequency ($\ln\sigma - \ln\omega$) for $x = 1.0$ (HDAF) at different temperatures. Lines are fit to (2), b) AC conductivity (σ') vs. frequency ($\ln\sigma - \ln\omega$) for $x = 0.8$ ($HDAF_{0.8}Z_{0.2}$) at different temperatures. Lines are fit to (2), c) AC conductivity (σ') vs. frequency ($\ln\sigma - \ln\omega$) for $x = 0.5$ ($HDAF_{0.5}Z_{0.5}$) at different temperatures. Lines are fit to (2), d) Exponent s vs. temperature T(K) for $x = 1.0$, arrows indicate transition temperatures, e) Exponent s vs. temperature T(K) for $x = 0.8$, arrows indicate transition temperatures, f) Exponent s vs. temperature T(K) for $x = 0.5$, arrows indicate transition temperatures, g) Exponent s vs. temperature T(K) for $x = 0.0$, arrows indicate transition temperatures.

To summarize, it can be seen that

1. Addition of 20% Zn causes a decrease in the 245 K transition temperature to 237 K. At 50% concentration of Zn this phase transition disappears. This could indicate that this phase transition is related to the two-dimensional nature of the Fe compound. As Zn reaches 50%, the extended layer formation is completely broken.
2. The (298 ±5) K transition is not really affected by the addition of Zn. Thus it is a characteristic transition related to the 2-D nature of the $FeCl_4$ planar structure.
3. Addition of Zn also affects the T_1 transition of HDAF, however it causes it to shift to higher temperatures by the first introduction of Zn. Further increase in Zn concentration does not seem to cause much change in the peak's position. This is reasonable in the light of the fact that this peak is related to a ferroelectric transformation.
4. The 255 K transition is related to the $ZnCl_4$ tetraheda, while the transition at 245 K is related to the 2-D nature of the material.
5. The conduction mechanism differs according to the temperature range investigated, as well as to the concentration. At high temperatures for Fe-rich concentrations, normal band type conduction prevails. For Zn-rich concentrations, series type conduction prevails as reflected by the "Jonscher regime".
6. At the lowest temperature, protonic-hopping type conduction takes place for $x = 0.5$, 0.8 and 1. Hopping of the chloride ions among vacant sites contributes to the conduction at low temperatures as well. It is not possible to be certain about the mechanism of conduction for HDAZ due to the many phase transitions observed in the low temperature region.

Conclusion

Introduction of Zn in place of Fe in the layered perovskite-like system results in

1. Increase in the number of observed phase transitions.
2. Decrease in the conductivity with increasing the Zn content.
3. Decrease in the activation energy of conduction in regions where Arrhenius relation is observed.
4. The conduction mechanism is affected by the introduction of Zn, where "series type" conduction is found for Zn-rich materials compared to normal band type conduction in Fe-rich materials at high temperatures.

[1] L. J. De Jongh and A. R. Miedema, Adv. Phys. **23**, 1 (1974) and references therein.
[2] M. F. Mostafa, R. Emrick, and A. S. Atallah, J. App. Phys. **81**, 4134 (1997).
[3] R. Kind. S. Plesko, H. Arend, R. Blinc, B. Zeks, J. Selinger, B. Lozar. J. Slak, A. Levstik, C. Filipic, V. Zaga, G. Lahajnar, F. Milia, and G. Chapuis, J. Chem. Phys. **71**, 2118 (1979).
[4] C. Courseille, N. Chanh, Th. Mars, A. Daoud, Y. Abid, and M. Laguerre, Phys. Stat. Sol. **143a**, 203 (1994).
[5] M. J. Tello, M. Arriendiaga, and J. Fernandez, Sol. Stat. Com. **24**, 299 (1977).
[6] C. Socfas, M. Arriendiaga, M. Tello, J. Fernandez, and P. Gilli, Phys. Stat. Sol. **57a**, 405 (1980).
[7] H. Kasano, N. Koshiji, and H. Mashiyama, J. Phys. Soc. (Japan) **61**, 346 (1992).
[8] A. J. Wolthuis, W. J. Huiskamp, L. J. De Jongh, and R. Carlin, Physica **142b**, 301 (1986).
[9] H. Kasano, N. Koshye, and Mashiycema, J. Phys. Soc. (Japan) **61**, 348 (1992).
[10] M. F. Mostafa, M. M. AbdelKader, A. S. Atallah, and M. El-Nimer, Phys. Stat. Sol. **135a**, 549 (1993).
[11] R. Jakubas, G. Bator, M. Foulon, J. Lefebvre, and J. Matuszewski, Z. Naturforsch. **48a**, 529 (1992).
[12] M. F. Mostafa and A. S. Atallah, Phys. Lett. **A264**, 242 (1999).
[13] M. F. Mostafa and S. S. Atallah, Sol. Stat. Comm. **117**, 69 (2001).
[14] P. B. Macedo, C. T. Moynihan, and R. Bose, Physics and Chemistry of Glasses **13**, 171 (1972).
[15] D. P. Almond and A. R. West, J. Non. Cryst. Solids **88**, 222 (1986).
[16] Ph. Colomban and J. C. Badot, Proton Conductors, ed. Ph. Colomban, C.U.P., Cambridge 1992.
[17] A. R. Long, Adv. Phys. **31**, 553 (1982).
[18] S. R. Elliott, Adv. Phys. **36**, 135 (1987).
[19] A. K. Jonscher, Dielectric Relaxation in Solids, Chelsea Dielectric Press, London 1983.
[20] H. Jain and J. N. Mundy, J. Non-Crystalline Solids **91**, 315 (1987).
[21] A. Pradel and M. Ribes, J. Non-Crystalline Solids **131–133**, 1063 (1991).
[22] W. K. Lee, B. S. Lim, J. F. Liu, and A. S. Nowick, Sol. Stat. Ionics, **53–56**, 831 (1992).
[23] B. S. Lim, A. V. Baysleyb, and A. S. Nowick, Appl. Phys. **A56**, 8 (1993).
[24] A. S. Nowick, B. S. Lim, and A. V. Baysleyb, J. Non-Crystalline Solids **172–174**, 1243 (1994).
[25] A. Pandit, B. Wankyln, T. Ansari, and R. Singh, Sol. Stat. Comm. **84**, 469 (1992).
[26] M. Pollak and G. E. Pike, Phys. Rev. Lett. **28**, 1449 (1972).